Electronic Supplementary Information:

Mixing mechanisms of lead nanoparticles with mineral particles: Implication of atmospheric transportation of lead

Yongpeng Ji[ab], Qiuju Shi[ab], Baocong Zhao[ab], Ziqi Wu[ab], Jiaxin Wang[ab], Weina Zhang[ab], Jiangyao Chen[ab], Yuemeng Ji[*ab], and Taicheng An[ab]

[a] Guangdong-Hong Kong-Macao Joint Laboratory for Contaminants Exposure and Health, Guangdong Key Laboratory of Environmental Catalysis and Health Risk Control, Institute Environmental Health and Pollution Control, Guangdong University of Technology, Guangzhou 510006, China

[b] Guangzhou Key Laboratory of Environmental Catalysis and Pollution Control, Key Laboratory for City Cluster Environmental Safety and Green Development of the Ministry of Education, School of Environmental Science and Engineering, Guangdong University of Technology, Guangzhou 510006, China

*Corresponding author: **Prof. Yuemeng Ji**

E-mail address: jiym@gdut.edu.cn

Additional details of the simulation

The simulation box for MD simulation is approximately 214 × 205 × 210 $Å^3$ in size. According to the ideal gas law (equation S1), there are 198 gaseous molecules in a simulation box with volume of 214 × 205 × 210 $Å^3$ at 298 K and 1 atm.

$$pV = nRT \quad \text{(S1)}$$

where p、V、n、R and T represent pressure, volume, amount of gaseous species, molar gas constant and temperature, respectively. The volume fraction of N_2 and O_2 in ambient condition are approximately 78% and 21%, respectively. Hence, 154 N_2 and 42 O_2 molecules were randomly inserted into the box to simulate the ambient air condition.

Furthermore, even with the high daily maximum atmospheric concentration for Pb of 1.3 μg/m^3 detected in Beijing,[1] the numbers for the molecule of Pb compounds is only 3.02 × 10^{-8} in the simulation box used in this study. Hence, to observe the mixing process and possible interaction between Al_2O_3 and Pb nanoparticles, the concentration of Pb nanoparticles used in this study is higher than that in ambient condition. And for each mixing system, four Pb nanoparticles were inserted into the simulation box.

The diffusion coefficients of Pb nanoparticles are calculated from their mean-square displacements according to the following relationship

$$x^2=2dDCt \quad \text{(S2)}$$

where x^2, d, DC, and t represent the mean square displacement, the dimension, the diffusion coefficient and the times, respectively. The mean-square displacement of Pb nanoparticles is analyzed using all trajectories of 3 ns simulation time.

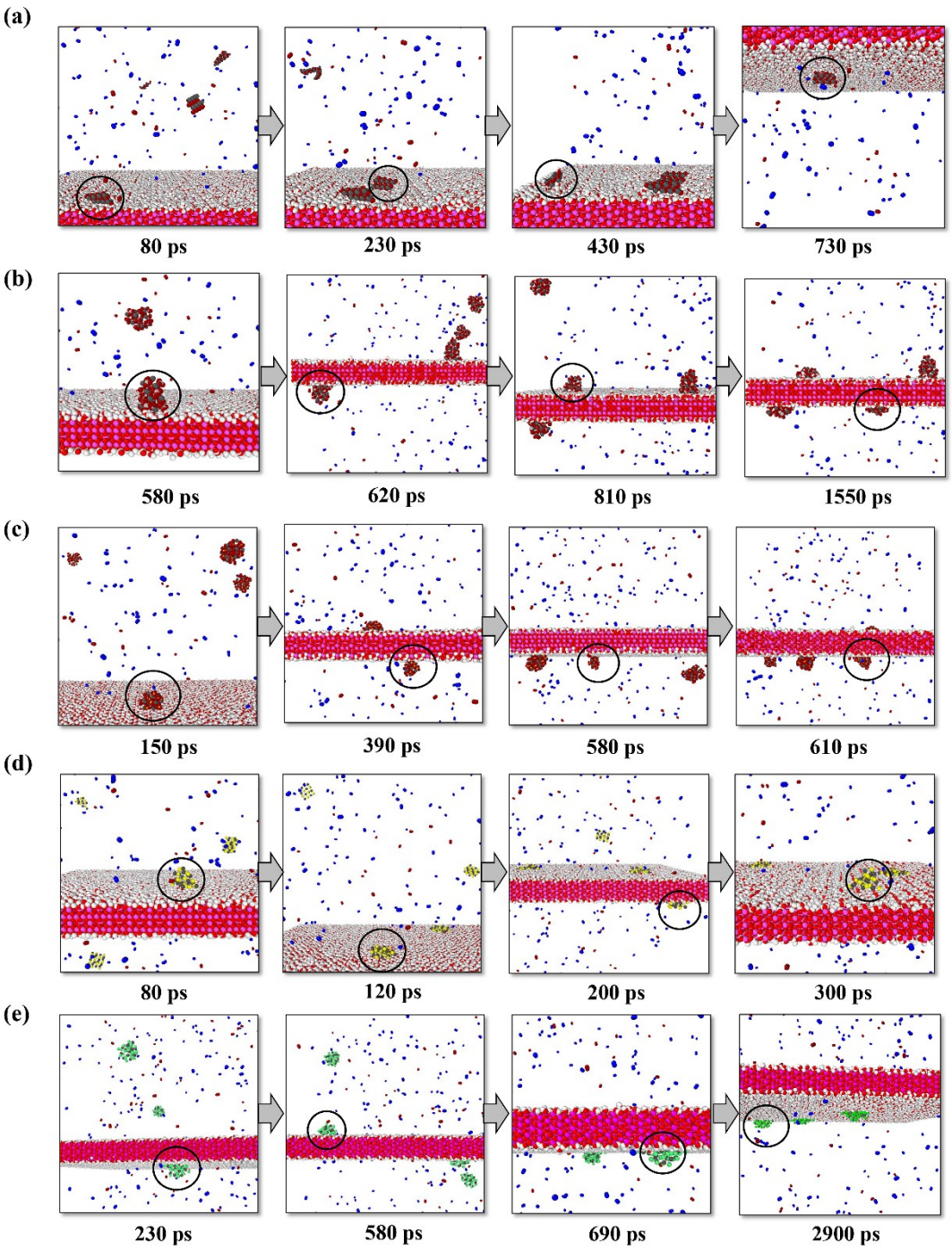

Figure S1. Representative trajectories for four Pb nanoparticles uptake onto Al_2O_3 surface in (a) PbO, (b) $PbCO_3$, (c) $PbSO_4$, (d) PbS and (e) $PbCl_2$ nanoparticle systems.

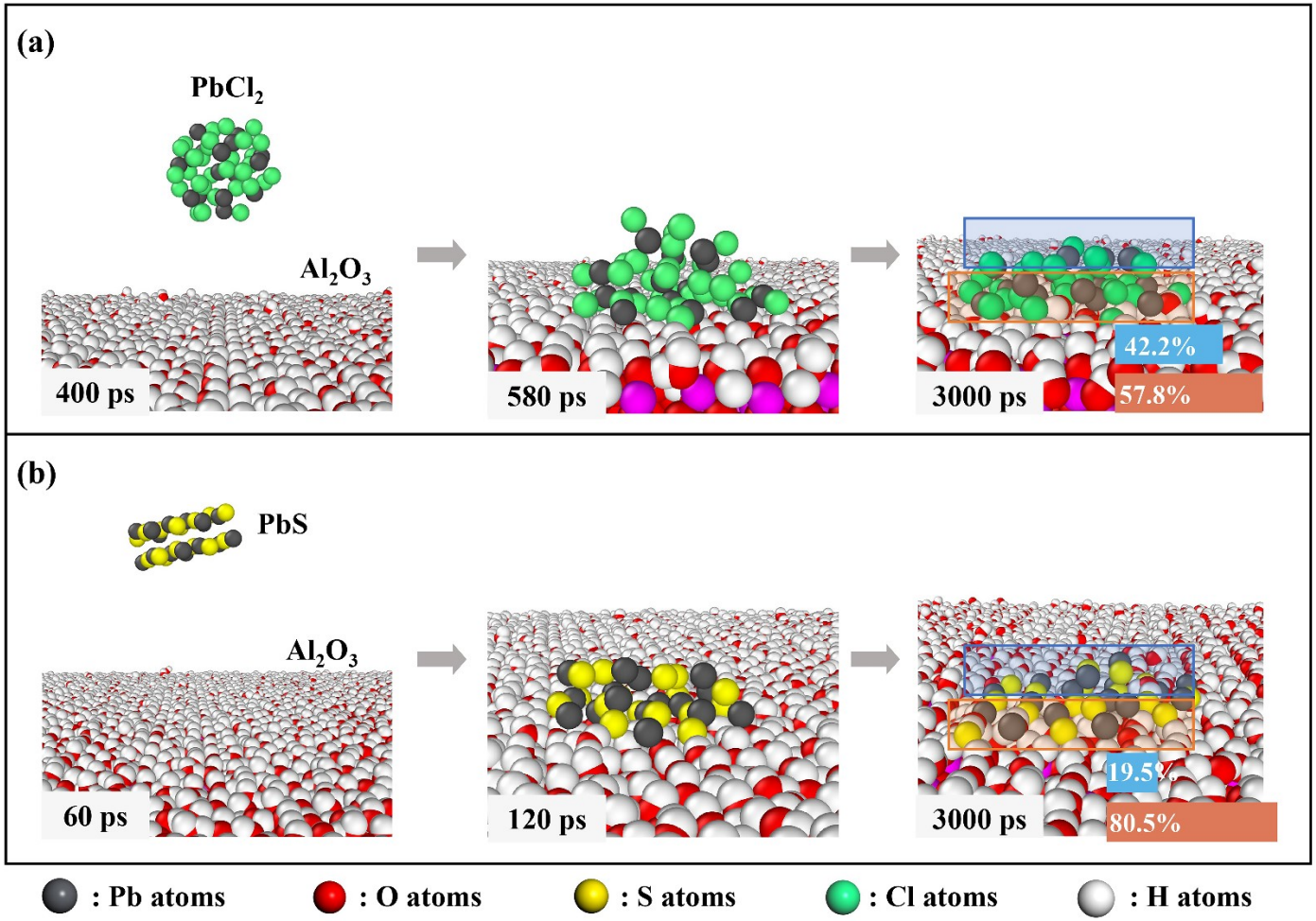

Figure S2. Selected snapshots of the MD trajectories for (a) $PbCl_2$, (b) PbS nanoparticle systems. Percentages are atoms in Pb nanoparticles that direct (orange area) and indirect (blue area) coordinate with Al_2O_3, respectively.

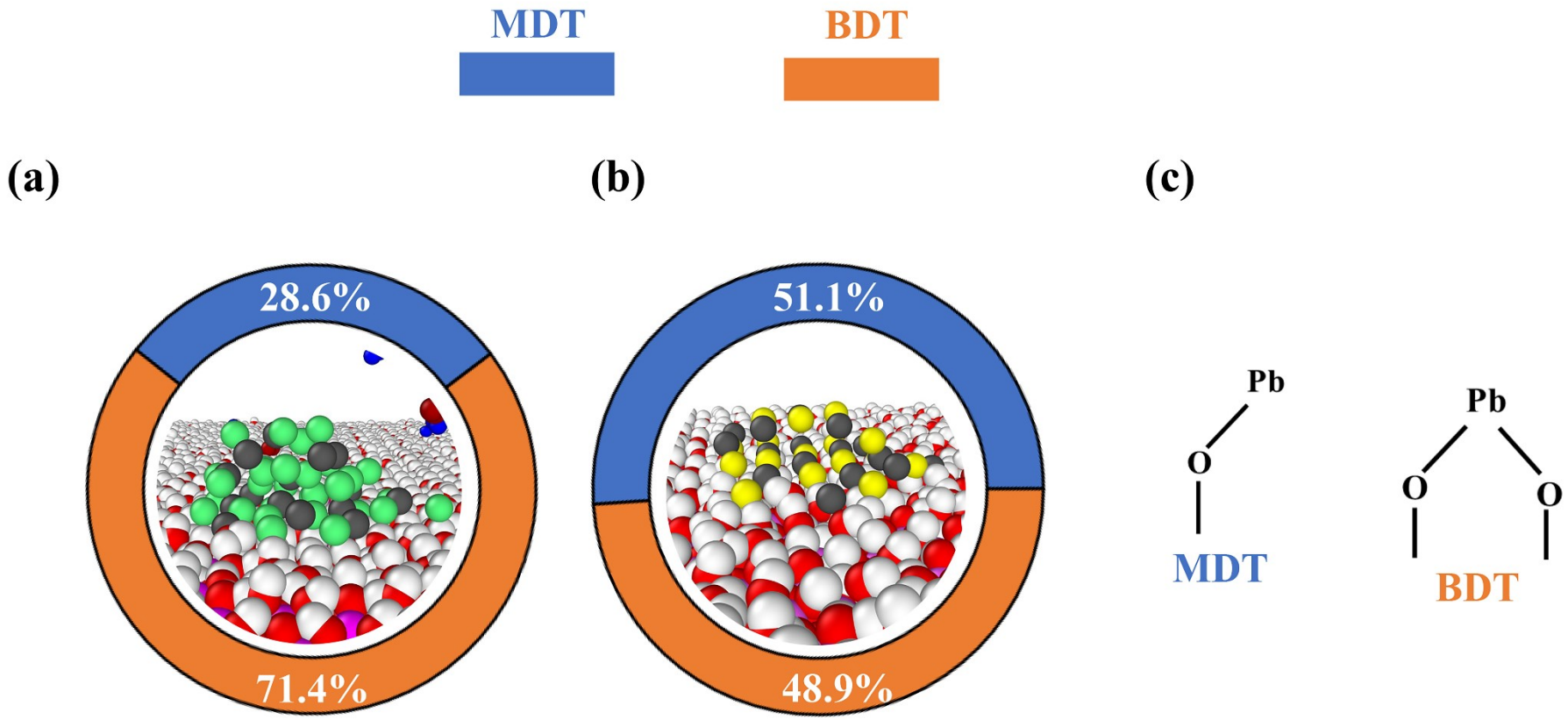

Figure S3. The branching ratios of the interfacial patterns between Pb nanoparticles with Al_2O_3 in (a) $PbCl_2$ and (b) PbS nanoparticle systems and (d) diagram for interfacial patterns of MDT and BDT.

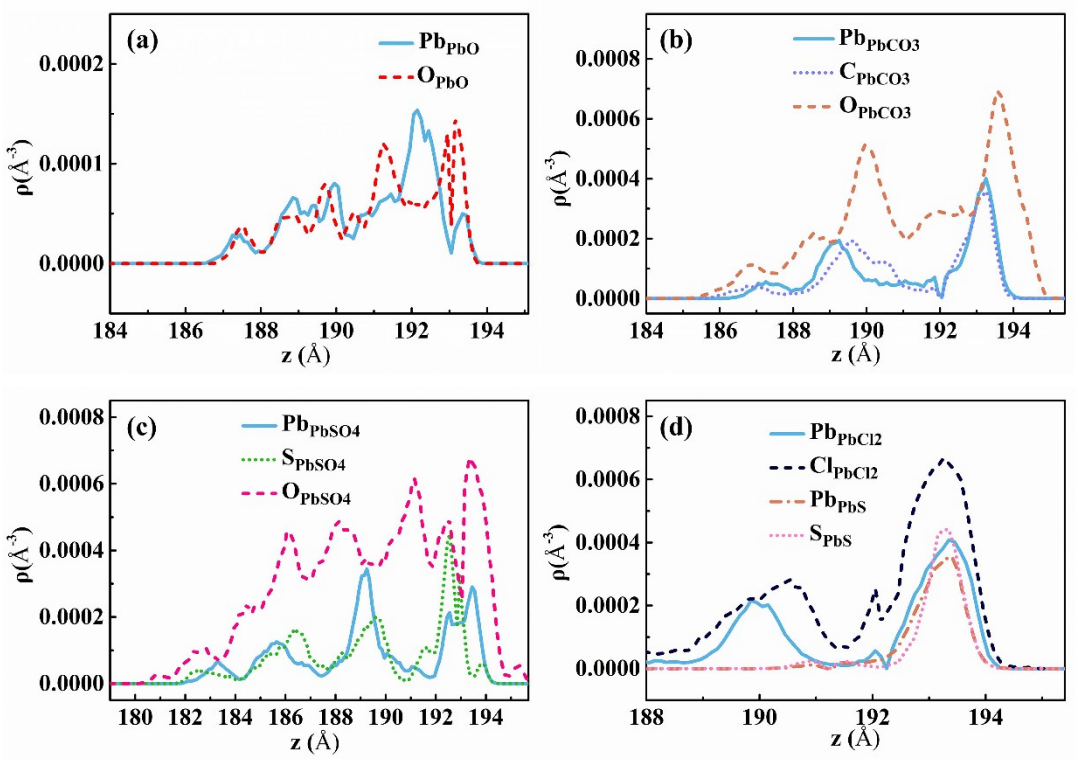

Figure S4. Atomic density profiles (ADPs) of Pb nanoparticles as functions of distance from Al_2O_3 surface for (a) PbO, (b) $PbCO_3$, (c) $PbSO_4$, (d) $PbCl_2$ and PbS nanoparticle systems. The mean positions for the H atoms of bottom Al_2O_3 surface are $z \approx 195$ Å.

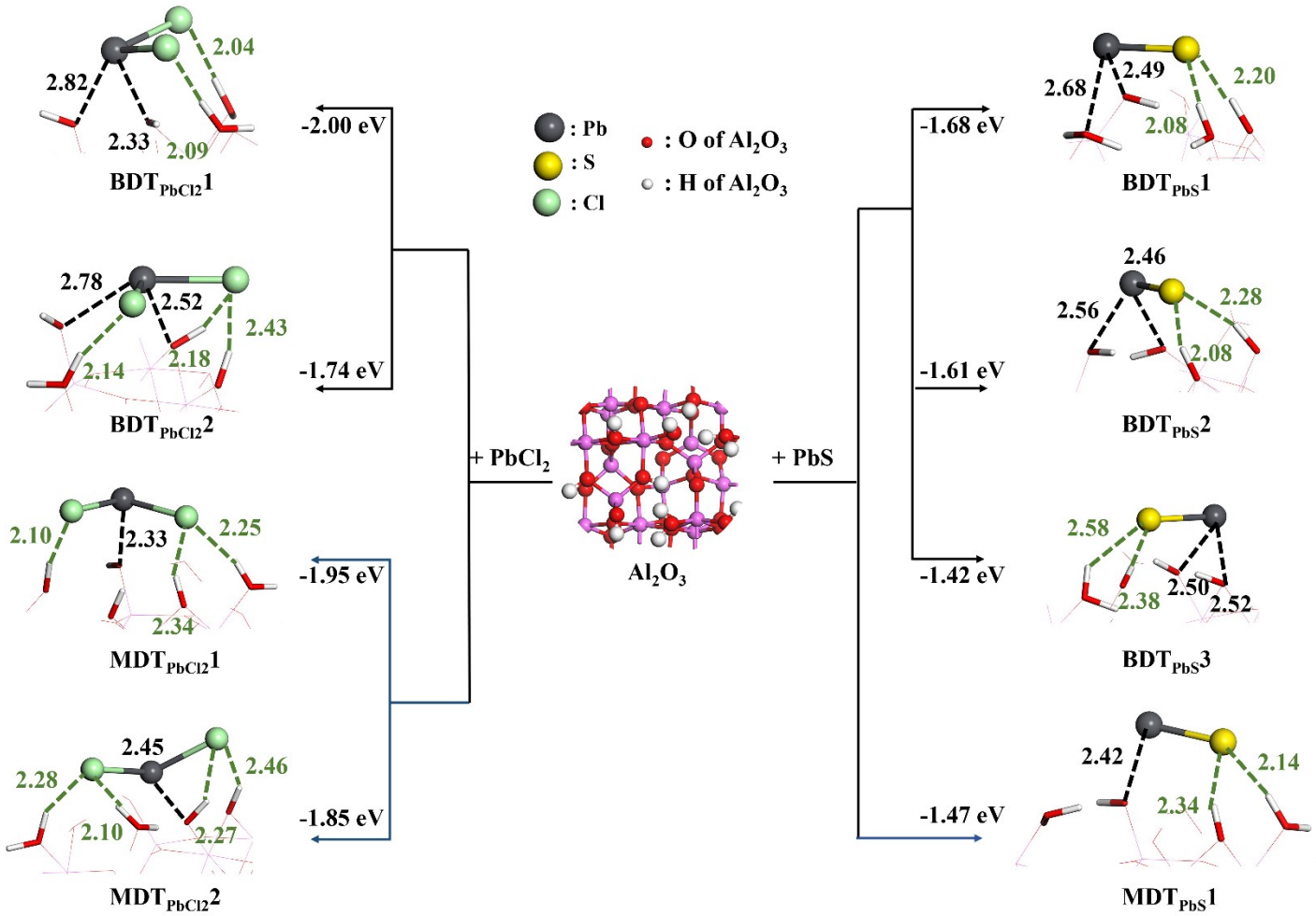

Figure S5. Potential energy surfaces of the mixing pathways in non-oxygenated Pb nanoparticle systems, along with the optimized geometries. The numbers in eV denote the mixing energies, and other numbers represent bond lengths in Å.

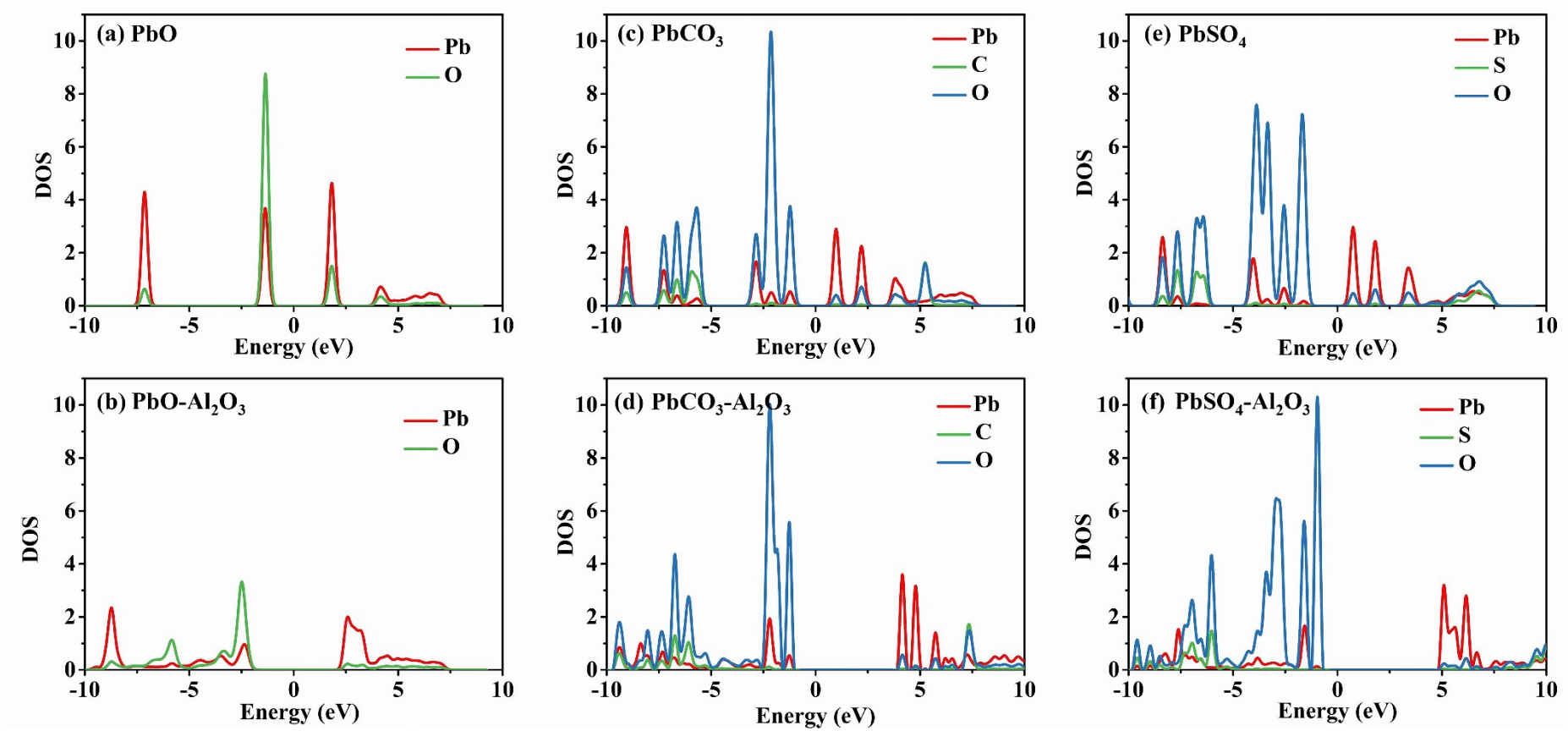
(a) PbO
Pb
O
(c) PbCO3
Pb
C
O
(e) PbSO4
Pb
S
O
(b) PbO-Al2O3
Pb
O
(d) PbCO3-Al2O3
Pb
C
O
(f) PbSO4-Al2O3
Pb
S
O
DOS
Energy (eV)
-10
-5
0
5
10
0
2
4
6
8
10

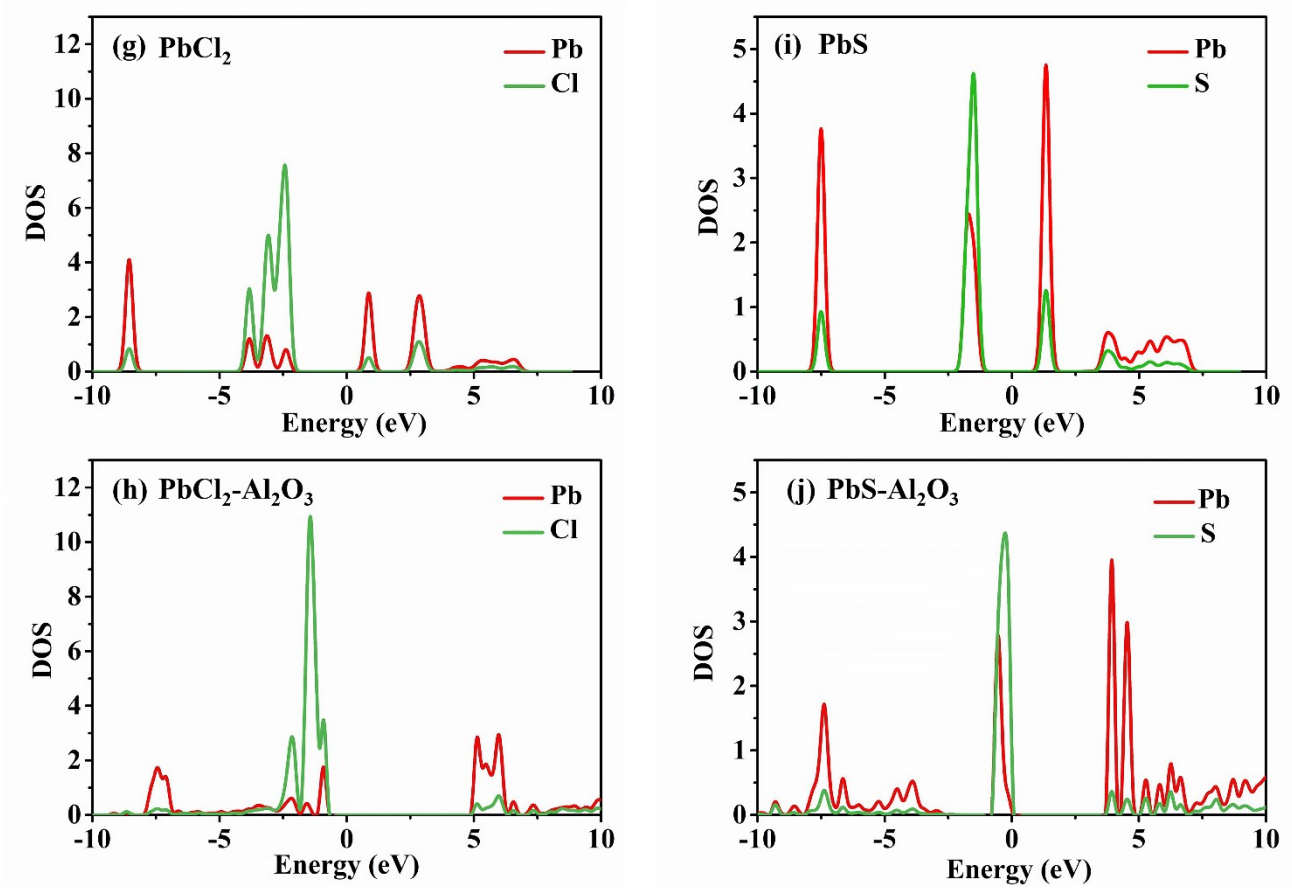

Figure S6. Density of states (DOS) for Pb molecules before and after mixing with Al_2O_3.

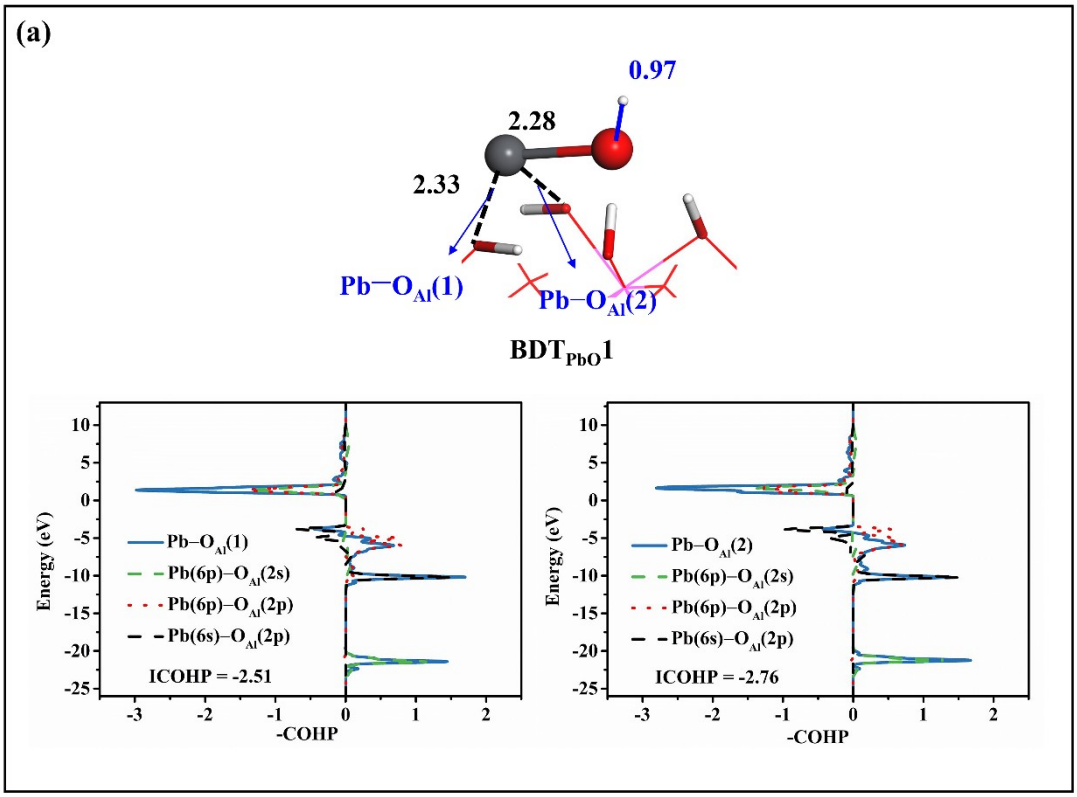

Figure S7a. Crystal orbital Hamilton populations (COHP) plots of heterocomplexes in (a) PbO, (b) $PbCO_3$, (c) $PbSO_4$, (d) $PbCl_2$ and (e) PbS nanoparticle systems.

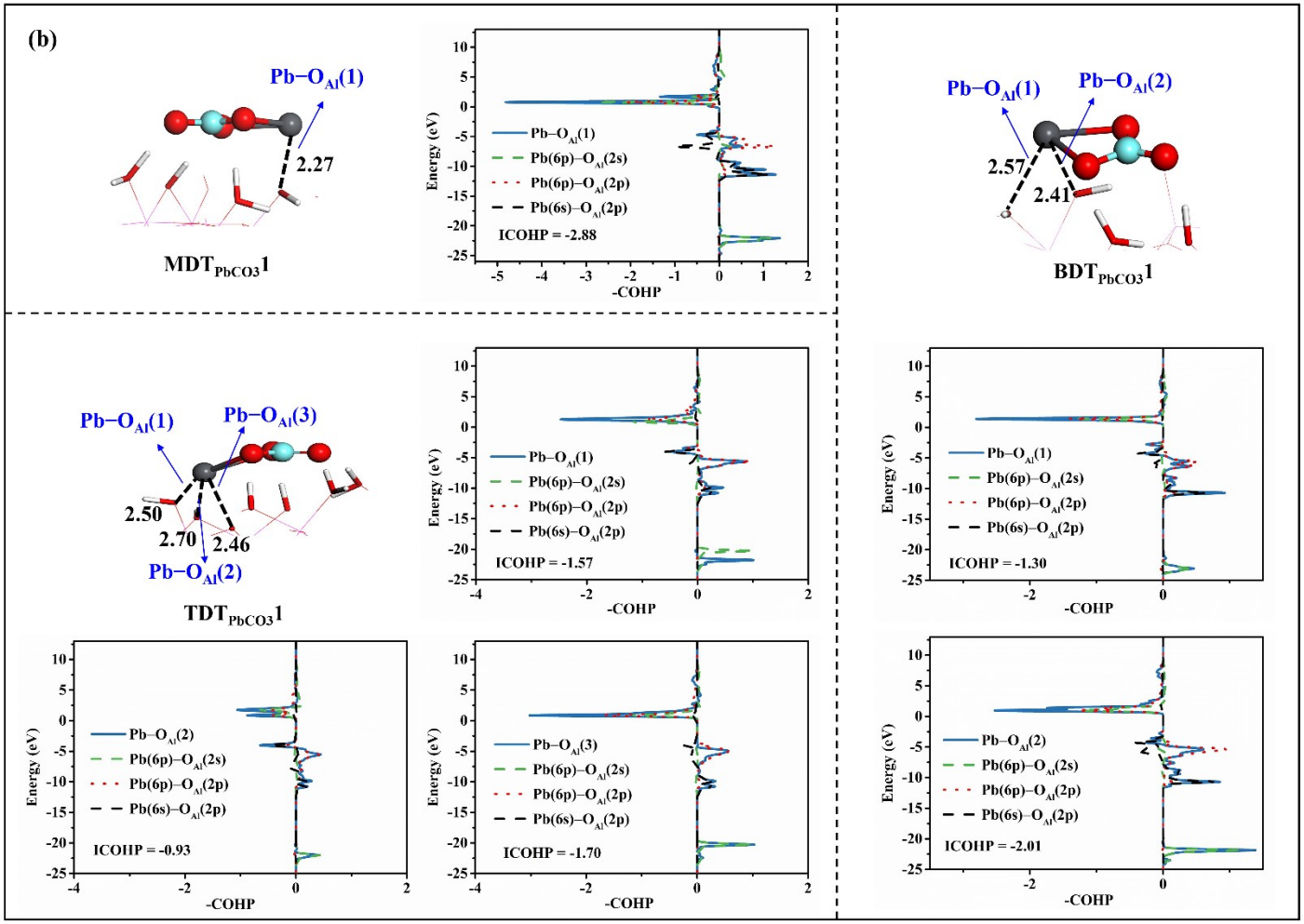

Figure S7b. Crystal orbital Hamilton populations (COHP) plots of heterocomplexes in (a) PbO, (b) $PbCO_3$, (c) $PbSO_4$, (d) $PbCl_2$ and (e) PbS nanoparticle systems.

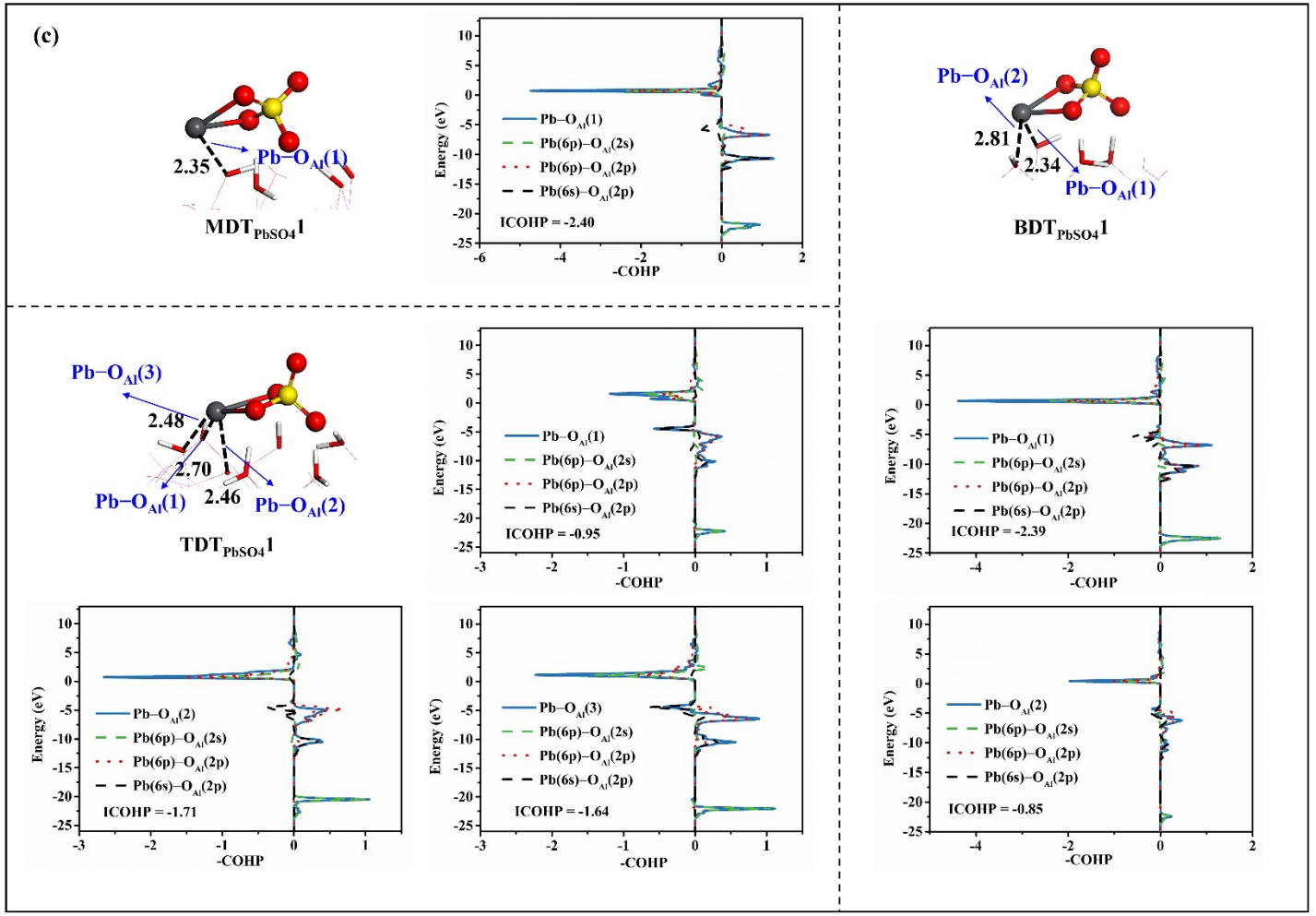

Figure S7c. Crystal orbital Hamilton populations (COHP) plots of heterocomplexes in (a) PbO, (b) $PbCO_3$, (c) $PbSO_4$, (d) $PbCl_2$ and (e) PbS nanoparticle systems.

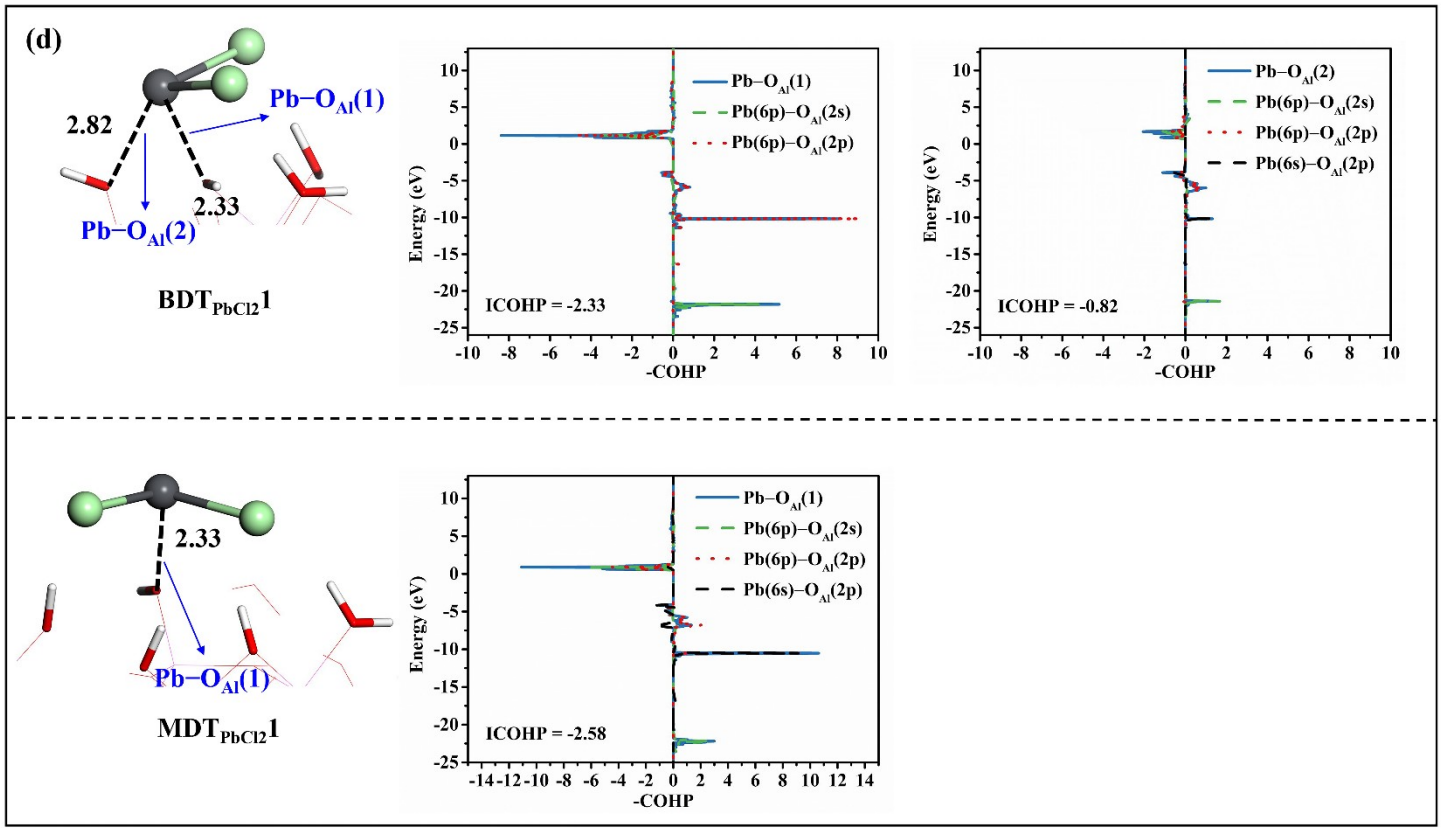

Figure S7d. Crystal orbital Hamilton populations (COHP) plots of heterocomplexes in (a) PbO, (b) $PbCO_3$, (c) $PbSO_4$, (d) $PbCl_2$ and (e) PbS nanoparticle systems.

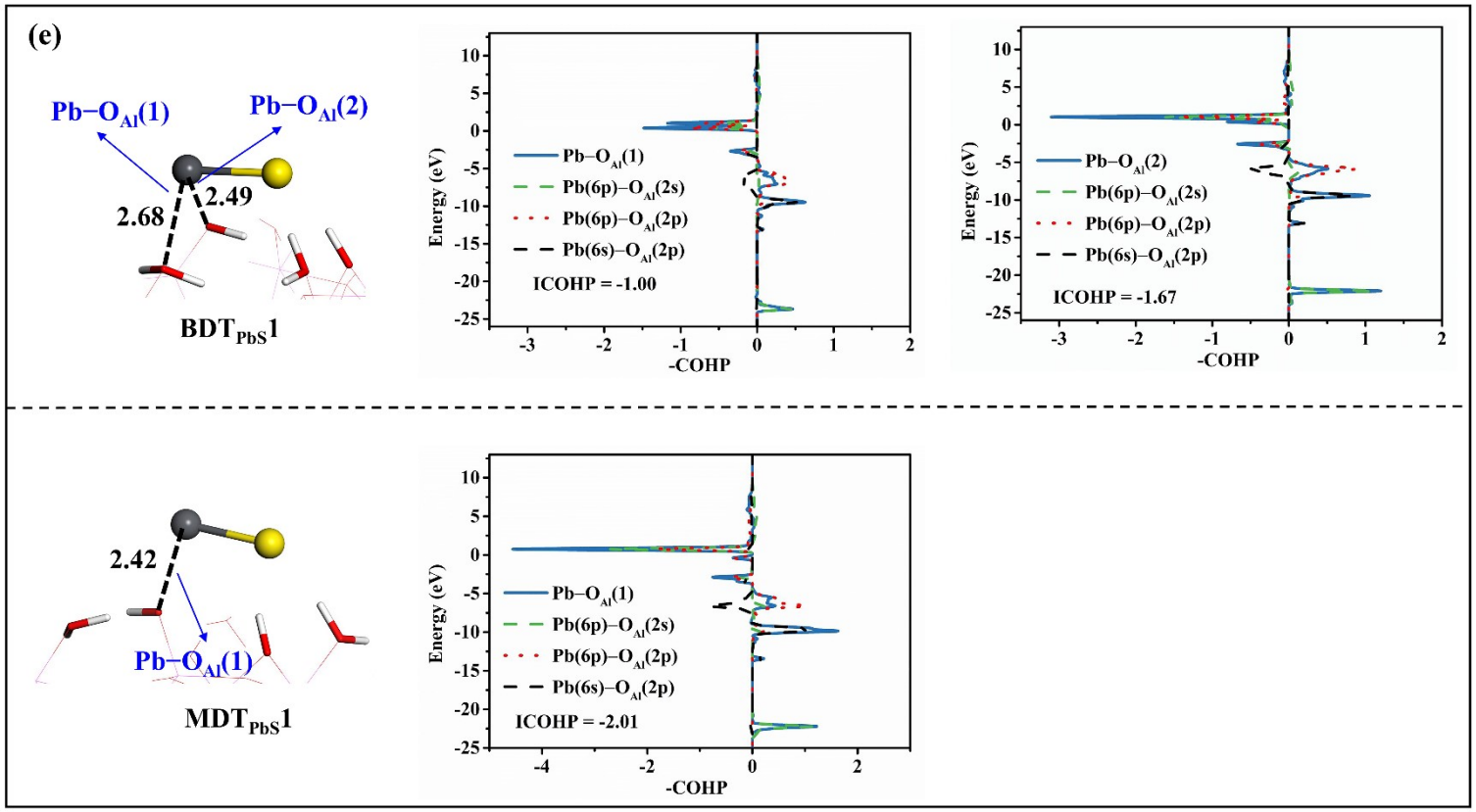

Figure S7e. Crystal orbital Hamilton populations (COHP) plots of heterocomplexes in (a) PbO, (b) $PbCO_3$, (c) $PbSO_4$, (d) $PbCl_2$ and (e) PbS nanoparticle systems.

Table S1. The integrated crystal orbital Hamilton populations (ICOHP) of Pb−O_{Al} in heterocomplexes.

ICOHP (eV)	Pb−O_{Al} (1)	Pb−O_{Al} (2)	Pb−O_{Al} (3)	Total-ICOHP
$BDT_{PbO}1$	-2.51	-2.76	-	-5.27
$TDT_{PbCO3}1$	-1.57	-0.93	-1.70	-4.20
$MDT_{PbCO3}1$	-2.88	-	-	-2.88
$BDT_{PbCO3}1$	-1.30	-2.01	-	-3.31
$TDT_{PbSO4}1$	-0.95	-1.71	-1.64	-4.30
$MDT_{PbSO4}1$	-2.40	-	-	-2.40
$BDT_{PbSO4}1$	-2.39	-0.85	-	-3.24
$BDT_{PbCl2}1$	-2.33	-0.82	-	-3.15
$MDT_{PbCl2}1$	-2.58	-	-	-2.58
$BDT_{PbS}1$	-1.00	-1.67	-	-2.67
$MDT_{PbS}1$	-2.01	-	-	-2.01

Table S2. Diffusion coefficients (*DC*s) of five airborne Pb nanoparticles (DC_{air}s) and five mixed Pb nanoparticles (DC_{mix}s) on Al_2O_3 surface at 298.15 K.

DC (m^2/s)	DC_{air} (m^2/s)	DC_{mix} (m^2/s)
$PbCl_2$	7.48×10^{-7}	2.40×10^{-9}
PbS	4.09×10^{-7}	4.49×10^{-10}
$PbCO_3$	6.54×10^{-7}	1.85×10^{-10}
$PbSO_4$	5.86×10^{-7}	1.59×10^{-10}
PbO	3.75×10^{-7}	1.25×10^{-10}

Reference

1 J. Cai, J. Wang, Y. Zhang, H. Tian, C. Zhu, D. S. Gross, M. Hu, J. Hao, K. He, S. Wang and M. Zheng, Source apportionment of Pb-containing particles in Beijing during January 2013, *Environ. Pollut.*, 2017, **226**, 30-40.